

## FEM Optimization of a Steel Belt of OTR Tyres

Jan Kledrowetz<sup>1,a\*</sup>, Jakub Javořík<sup>2,b</sup>, Rohitha Keerthiwansa<sup>3,c</sup>,  
Pavel Kratochvil<sup>4,d</sup>, Soňa Rusnáková<sup>5,e</sup> and Petr Gross<sup>6,f</sup>

Tomas Bata University in Zlin, Faculty of Technology, Vavreckova 275, 760 01 Zlin,  
Czech Republic

kledrowetz@utb.cz

**Keywords:** Tyre, rubber, steel cords, composite, optimization, cracks, FEM, MSC Marc/Mentat

**Abstract.** This paper deals with an FEM simulation of a steel belt of tyres. A belt is a part of a tyre that plays a very important role in all radial tyres especially in case of heavy-duty off-the-road (OTR) ones. It is a composite composed of rubber material and a steel reinforcement. High peak stress inside this composite can initiate cracks, which subsequently lead to a complete tyre failure. In this work, the belt is extracted from the tyre and simulated separately in order to be able to cover individual cords. Belt behaviour under tension is studied and optimal cord distribution is proposed to decrease the risk of the failure. FEM software MSC Marc/Mentat is employed as a calculation tool.

### Introduction

A pneumatic tyre is a complex composite product that consists of different rubber materials, textile or steel cords and steel wires. OTR (Off-the-road Tyres) are built to take a huge amount of weight and roll through conditions that would stop other vehicles dead. They are mainly used in earthmoving, mining or civil industries for OTR applications.

The simulations were performed in MSC Marc. MSC Marc is one of the best software in the world capable of dealing with nonlinear analyses with advanced algorithms for solving contact problems and highly nonlinear materials, as rubber-like materials. It also provides a capability to model accurately reinforcing parts as carcass or belt layers using a special tool developed for this purpose, so called rebar elements. MSC Marc is a finite element method (FEM) software. Basic principle is to discretize a complicated and nonlinear problem into element with simple solution. It is based on Lagrange's principle: a body is in a state of equilibrium, if the total potential energy of a system is minimal. Marc has an implicit solver that is suitable mainly for static or steady state analyses [1].

The major parts of an all-steel OTR tyre are following [2]:

- **Tread** – contains a massive tread pattern and is the tyre contact point to the ground.
- **Sidewall** – protects the casing ply from mechanical and environmental effects.
- **Innerliner** – inner layer of the tyre that maintains the inflation pressure.
- **Apex** – is located above the bead wire to fill the gaps between the carcass plies.
- **Bead Wire** – holds the tyre tightly on the rim without any slippage.
- **Carcass** – stiff layers of steel cords that are laid at an angle close to 90° to the centreline of the tread. Carcass layers connects the bead bundles with each other. It shapes the tyre profile and transfers contact forces to the belt.
- **Belts** – layers of steel cords that are laid at a small angle to the centreline of the tread and are located under the tread. Builds the vertical stiffness of the tyre in cooperation with air pressure and generates longitudinal, lateral, and cornering stiffnesses.



Fig. 1: A typical OTR tyre [3]

If the belt is not designed properly, it often leads to initiation and propagation of cracks and subsequent failure of the entire tyre (fig.2).



Fig. 2: Destroyed tyre due to the initial cracks in the belt region

Cracking of rubber can be initiated at or near an interface with a tyre cord. Such cracking may progress around the cord itself, creating a condition called socketing. Continued crack growth can result in smaller cracks meeting one another and progressing further. Fracture of cords or filaments can lead to structural weakness that causes a whole-tyre rupture or leads to more slowly developing internal ply separation, depending on the extent of the damage. [4]

### Numerical Model

Numerical models are composed of a mesh of elements [5]. The type of elements and density of the mesh are also very important. Element mesh density has also a significant impact on the results. The mesh is required to be dense enough, mainly in the places around and between the cords. [6]

**Entire tyre.** A pneumatic tyre is a complex composite product that consists of different rubber materials, reinforcing cords and steel wires in the beads. Rubber materials are mathematically described by hyperelastic models. MSC Marc allows to use more than 10 different models in the 2019 version.

Reinforcement cords can be represented through rebar elements. They are hollow line (2D) or surface (3D) elements in which cord properties might be defined, such as end-count, orientation, cross-section area, material properties, micro-buckling behaviour in compression, etc. The reinforcing cords that are modelled by the rebar elements are assumed to be in the form of layers. Cords are embedded in matrix elements. Each layer of reinforcement cords is smeared into an

equivalent layer with a uniaxial stiffness in the reinforcement direction. Numerical integration to form the element stiffness is carried out over this rebar layer and not over individual cords [1]. This is a very effective way of modelling the reinforcement in the entire tyre.

**Single belt.** Including individual cords would be very time consuming and computationally impossible using the current HW. Therefore, this model was used just for studying overall belt behaviour. Then, the belt was extracted from the tyre and reinforcement was modelled using individual cords. Appropriate boundary conditions were derived from the overall tyre behaviour.

Rubber material was described by the Neo-Hookean hyperelastic model [5]. Its parameters were calculated from three different measurements: uniaxial tension, biaxial tension and pure shear [7,8]. C01 Parameter of the coating rubber was  $C01 = 0.40$ . Measured Young modulus of the steel cord was 116 GPa.

**Crack propagation.** MSC Marc is capable of simulating crack propagation with the fracture mechanics option. It covers the evaluation of energy release rate and J-integral including automatic crack propagation using two methods: the mode separation method with the Lorenzi option and the Virtual Crack Closure Technique (VCCT) through VCCT option. The VCCT option also supports automatic crack propagation. At the beginning, existence of a crack is presupposed. When material is loaded, conditions under which crack growth occurs are examined.

The basic concept presented by Griffith and Irwin is an energy balance between the strain energy in the structure and the work needed to create a new crack surface. This energy balance can be expressed using the energy release rate as:

$$G = G_C \quad (1)$$

G is defined as

$$G = -\frac{d\Pi}{da} \quad (2)$$

Where

$\Pi$  is the strain energy,

a is the crack length,

$G_C$  is the fracture toughness of the material. This property is determined from experiments. [1]

G depends on the geometry of the structure and the current loading. Equation (1) is used as a fracture criterion – a crack starts to grow when:

$$G > G_C \quad (3)$$

In the simulations in this study the VCCT option was employed. The VCCT option offers a general way for obtaining the energy release rate. The implementation follows the description in R. Krueger [8].

## Methods

**Stress analyses.** To generalize the results, the model was axisymmetrical and steel cords had  $0^\circ$  angle (so they were circumferential).

When the studied tyre was inflated to its nominal pressure 1000 kPa, the belt grew by 1 mm on tyre radius. Hence, the bottom edge of the belt layer was moved radially by this distance. One of the basic characteristics of the rubber is that it is incompressible. Therefore, the side and top edges were set free, hence when the thickness decreases, the width must increase. Nevertheless, in the real service condition, the belt is embedded in the rubber, so this movement is partly limited. Therefore, the belt strip was modelled very wide and stress was recorded only in the middle of the width.

Since the overall end-count of the cords was studied, not the effect of the construction of the cord, steel cords were modelled as wires. Single yarns were neglected. In this analysis, there was a perfect contact between the cords and the rubber.

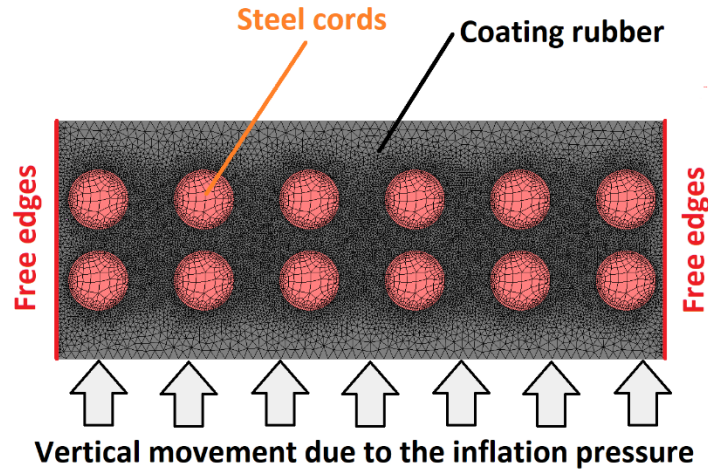


Fig. 3: FE model used for this study

To make the end-count independent on the cord diameter, the distance between the cords was defined as (fig. 4):

$$S = \frac{D}{d} \quad (4)$$

Distance between the layers A was constant, where

$$A = \frac{d}{3} \quad (5)$$

The ratio S was ranged from 0.0625 to 2.3.

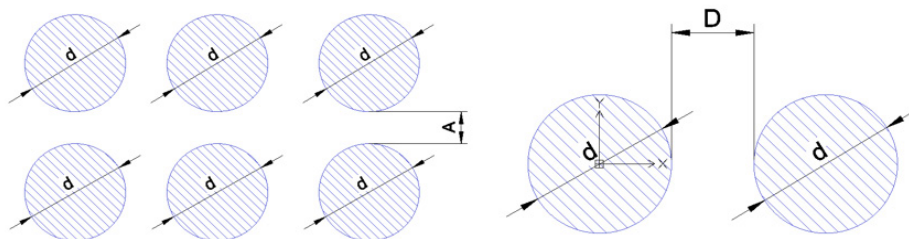


Fig. 4: Drawing of the belt configuration where only D is a variable

Maximal stress between the cords was recorded for each configuration.

**Crack propagation.** When the tyre is rolling, the belt is stressed by a cyclic load. This type of loading was modelled as a periodical increase and decrease of the bottom edge diameter. This led to material fatigue and subsequent crack propagation.

In the first step, the initial crack was always put into the location of the highest stress, which was determined by the previous analyses. If the stress around the crack tip was sufficient, i.e. the criterion (3) was fulfilled, then the crack growth was performed. Cracks grew at the end of each fatigue time period. Also, contact between the rubber and the cords was changed to glued with separation. So, when the critical stress was reached, the separation of the two components happened.

The goal here was to find out how much and along which trajectory cracks propagate. Exact number of cycles, when cracks start to propagate was not the aim of this work.

## Results

**Stress analyses.** There were seven different D/d configurations calculated. For each configuration, maximal Cauchy stress at the cord-rubber interface, between the cords in the same layer and between the cords in the adjacent layer (between vertical cords in these simulations) were recorded. Since

initiation of the cracks was inside the rubber, stress in the cords was not studied in this work. Stress distribution of all the versions is shown in fig.5.

The stress scale is different for each figure in order to be able to clearly read the stress map. For a better comparison, it would be better to keep the same scale, but for low end-counts, where stress is much lower, the stress map would spread into one or two colours. Stress scale is always located on the left side of each picture.

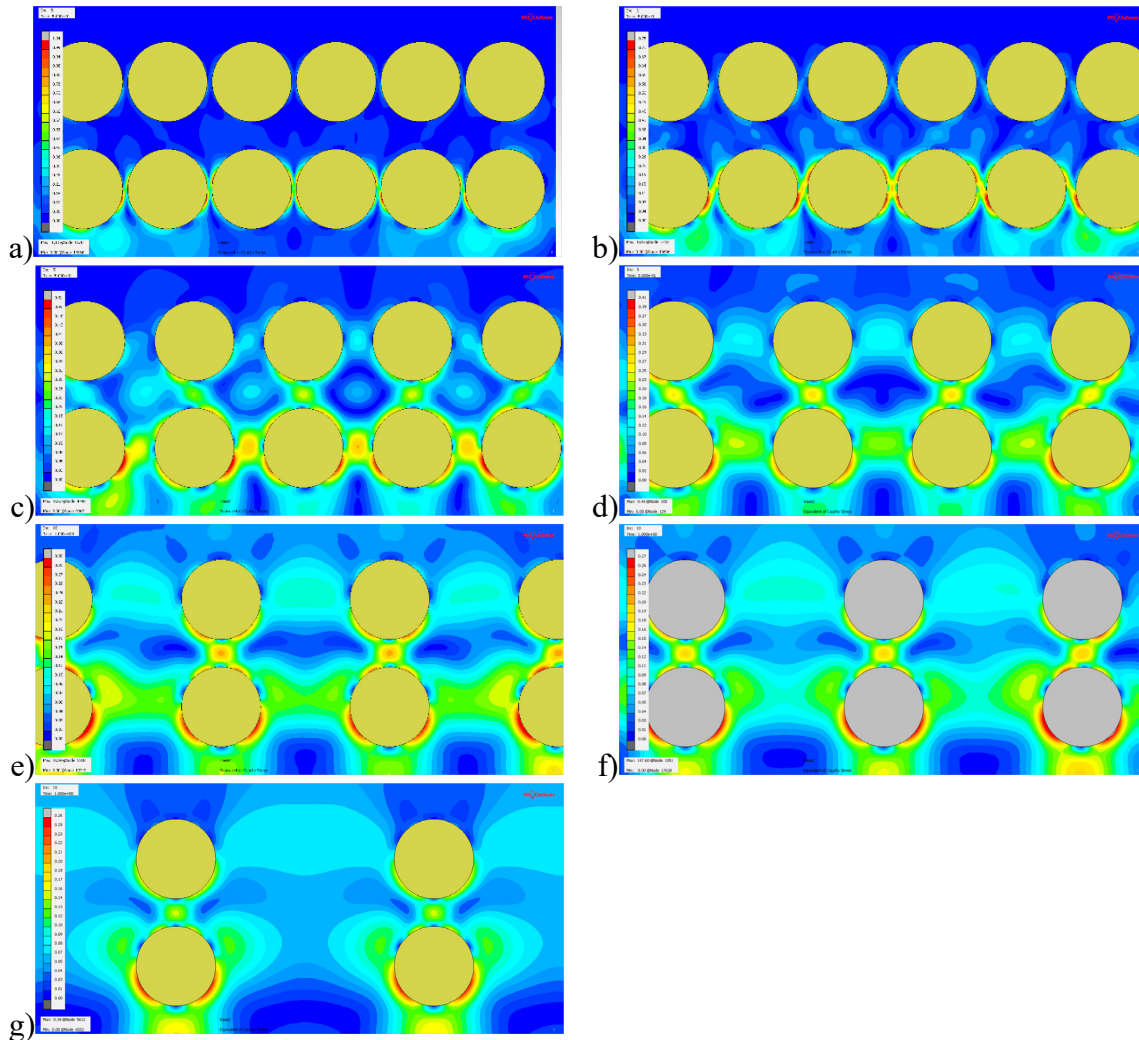


Fig. 5: Cauchy Stress in the rubber around the cords under different end-count

Peak stress values from each configuration were recorded into the table (1).

Table 1: Calculated stress in different parts of the belt strip

D/d	Stress interface [MPa]	Stress between the cords in the same layer [MPa]	Stress between the cords in the adjacent layer [MPa]
0.063	1.04	0.56	0.09
0.125	0.75	0.58	0.17
0.415	0.51	0.39	0.30
0.800	0.41	0.23	0.27
1.125	0.30	0.14	0.24
1.550	0.27	0.10	0.20
2.300	0.26	0.06	0.15

The dependence of the D/d on the maximal Cauchy stress was also plotted into a graph and regression of the values was performed. The results are shown in the graph below (Fig. 6).

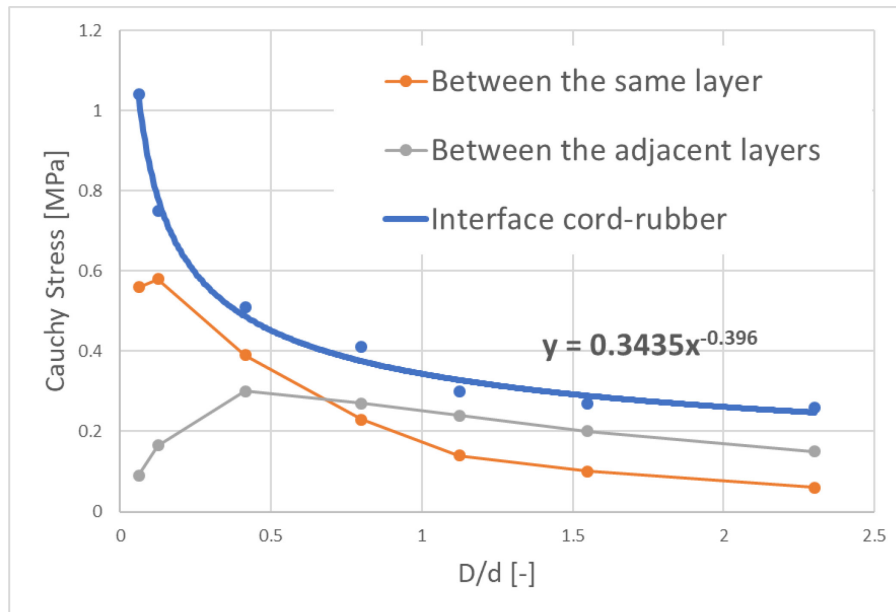


Fig. 6: Dependence of the stress in different locations in the coating rubber on D/d parameter

From the presented results, the following is obvious:

- For all D/d range, the maximal stress is in the cord-rubber interface
- For low D/d, there is another local maximum between the cords in the same layer (e.g. fig.5c)
- When D/d increases, a local maximum between the cords in the adjacent layers occurs (e.g. fig.5e)
- Dependence of D/d on maximal Cauchy stress is exponential with the fitting equation  $y = 0.3435 \cdot x^{-0.396}$ .
- Stress between the cords in the same layer decreases with higher D/d ratio
- Stress between the cords in the adjacent layer rises and reach its maximum at around D/d = 0.4, then it decreases parallelly with the stress in the other two locations.
- For low D/d, local maximum between the cords in the same layer is higher. But from D/d=0.6, stress between the adjacent layers turns to higher values.

**Crack propagation.** All of these configurations were taken and subjected to fatigue calculations.

For configurations, where  $D/d > 0.415$ , initial crack propagated either very little (did not reach other cords) or did not propagate at all. When  $D/d \leq 0.415$  crack propagated to the other cords.

Example of the crack propagation procedure for  $D/d = 0.125$  is shown in the following figure (7).

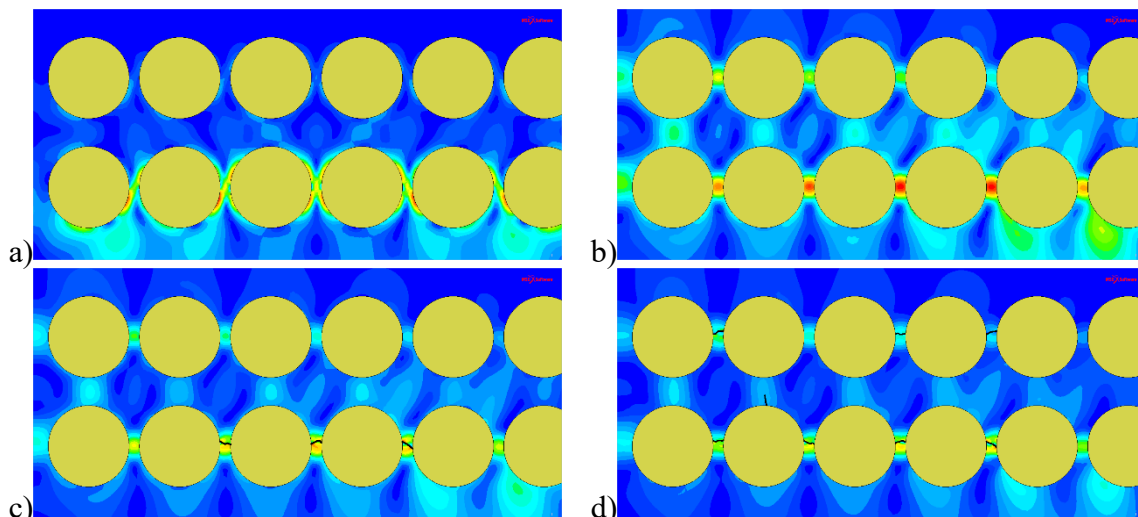


Fig. 7: Crack initiation and propagation in the simulation when D/d = 0.125.

The crack proceeded as following:

- a) This was the stress state from the previous analysis. The belt strip was stretched without the cracks at this moment. Maximal stress was at the interference cord-rubber in the bottom side part of the cords.
- b) After some number of cycles, cords lost their adhesion to the coating rubber and separated. First, at the location of the highest stress, then spread to the rest of the cord circumference. This separation caused significant changes in the stress distribution.
- c) From now, cracks began to propagate between the cords in the same layer. When rubber area between two cords was completely separated by a crack, stress was immediately transmitted to the other regions, where stress rose immediately and cracks started to propagate.
- d) At the end, whole belt layer was separated from the adjacent layer and the cracks could further propagate to the other region as sidewall or tread causing ultimate failure of the tyre.

### Discussion

It is obvious, that the cord spacing has a significant influence on stress in the surrounding rubber as well as on crack initiation and propagation.

Without thinking about the inside stress, one would probably choose as high end-count (small  $D/d$ ) as possible in order to increase the stiffness of the belt. But this would probably mean high stress, hence earlier failure. On the other hand, if the goal was just to decrease the stress and increase the crack resistance, one would go for lower end-count, i.e. high  $D/d$  ratio to decrease the risk of failure. On the contrary, this would make the belt layer very soft and many of them would have to be applied to maintain the overall belt strength.

The most convenient solution is, obviously, somewhere in between. Due to the fact, that the dependence of  $D/d$  ratio on the stress is exponential, values in the area of high slopes should be avoided. Such configurations generate high stress. Production inaccuracies must be also considered. When  $D/d$  would be in the high-slope area, small variations in the production could mean significant stress magnitude variations.

When studying the fracture mechanics, from around  $D/d = 0.6$  cracks do not propagate significantly, for even higher ratios, cracks do not propagate at all.

All in all, it is recommended that  $D/d$  ratio higher than 0.6 is used.

### Summary

It is obvious, that the cord spacing has a significant influence on stress in the surrounding rubber as well as on crack initiation and propagation.

$D/d$  ration must be selected carefully, since its dependence on stress is exponential. The ratio should not drop below 0.6 where the slope of the exponential curve starts to increase rapidly and cracks start to propagate to the surrounding area. On the other hand, the ratio must not be too high because the belt would become very soft. Certainly, the most suitable ratio depends on more factor such as tyre application, tyre dimension and construction, tyre load, safety factor of all belts, etc. In real tyres, the belt layers often have different construction, where only the most critical ones can be optimized to avoid cracking.

Further improvement might be brought by applying the real cord angle including the correct expansion rule and by modelling the cords with detailed construction, e.g.  $7 \times 7 \times 0.25$ . However, these calculations would be very demanding on HW and the results would be probably connected only to the particular configuration.

### Acknowledgment

This work and the project is realized with the financial support of the internal grant of TBU in Zlín No. IGA/FT/2019/001 funded from the resources of specific university research.

---

**References**

- [1] Information on <https://simcompanion.mscsoftware.com/infocenter/index?page=home>.
- [2] J.Kledrowetz, J. Javořík, G.W.R. Keerthiwansa and P. Nekoksa, Calculation of the tyre curing mould cavity shape using FEM, *Manufacturing Technology*, Volume17, Issue 4, 2017. Pages 479-483, ISSN 1213-2489.
- [3] Information on <https://www.mitas-tyres.com/international/products/em-mpt-industrial-tyres/>
- [4] A.N. Gent, J.D. Walter, *The Pneumatic Tire*. Washington, D.C.: NHTSA, 2005.
- [5] Nonlinear finite element analysis of elastomers, [ebook] MSC Software. Available at: [http://www.mscsoftware.com/assets/103\\_elast\\_paper.pdf](http://www.mscsoftware.com/assets/103_elast_paper.pdf) [Accessed 29 Oct. 2019].
- [6] J. Kledrowetz et al., FEM Modelling Techniques for Three Point Bend Test of Rubber Composites, *Materials Science Forum*, Vol. 919, pp. 257-265, 2018
- [7] J. Javorik, Z. Dvorak, Equibiaxial test of elastomers. In *German Rubber Conference 2006*. Nuremberg. Germany. Deutsche Kautschuk-Gesellschaft e.V., 2006. p. 297-299.
- [8] R. Keerthiwansa et al., "Hyperelastic Material Characterization: A Method of Reducing the Error of Using only Uniaxial Data for Fitting Mooney-Rivlin Curve", *Materials Science Forum*, Vol. 919, pp. 292-298, 2018
- [9] R. Krueger, Virtual Crack Closure Technique: History, Approach and Applications, *Appl. Mech. Rev.*, Vol. 57:2, pp. 109–143, March 2004.